

## PERFORMANCE EVALUATION OF WIRE SPRING FIN FOR COMPACT PLATE-FIN HEAT EXCHANGERS

H. Iwai<sup>1</sup>, S. Kawakami<sup>2</sup>, K. Suzuki<sup>3</sup>, J. Tsujii<sup>4</sup> and T. Abiko<sup>5</sup>

<sup>1</sup> Kyoto University, Kyoto, Japan, iwai@mech.kyoto-u.ac.jp

<sup>2</sup> Kyoto University, Kyoto, Japan, souchi@t01kougakubu.mbox.media.kyoto-u.ac.jp

<sup>3</sup> Shibaura Institute of Technology, Saitama, Japan, ksuzuki@sic.shibaura-it.ac.jp

<sup>4</sup> Sumitomo Precision Products Co., LTD., Amagasaki, Japan, tsujii@spp.co.jp

<sup>5</sup> Sumitomo Precision Products Co., LTD., Amagasaki, Japan, abiko-t@spp.co.jp

### ABSTRACT

Use of thin metal wire structures as a new type of extended heat transfer surface is proposed. As one of the most basic structure of this kind, the heat transfer performance of a spring shaped fin is experimentally investigated under relatively low Reynolds number conditions ( $100 < Re_{dh} < 1000$ ). Averaged heat transfer coefficient is evaluated by modified single-blow method while the pressure drop is measured at a steady state flow condition. The effects of the geometric parameters such as wire diameter, spring pitch and pitch ratio were systematically examined and the obtained data were compared with that of a conventional offset fin, which is commercially available. It was found that the geometric parameters of the spring fins and the arrangement of spring fins in the test section affect their performance. Some types of spring fins showed better heat transfer performance than a conventional offset fin, if they are evaluated in terms of the total heat transfer at a constant pumping power.

### INTRODUCTION

Development of a high temperature effectiveness compact heat exchanger that can be used under high temperature conditions is one of the important requirement from distributed energy systems (Suzuki et al., 2003) like micro gas turbine, high temperature fuel cell systems etc. There are two major streams in developing such heat exchangers, one is primary surface type and the other is plate-fin type. Primary surface types have a potential to achieve the demanding requirements at relatively low cost as they do not need brazing process and therefore intensive investigations are recently going on (McDonald, 2000, Iwai et al., 2003). Plate-fin types, on which this study focuses, have been being investigated for decades and the

accumulated information is available in handbooks and literature. For further evolution of plate-fin types, a development of effective fin geometry would be a key.

Applying porous materials, such as formed metals, as extended surface to compact plate-fin heat exchanger (Kim et al., 2000) is one of the interesting options recently proposed. It is an attractive and probably effective way to enhance heat transfer because of its large surface area density. The materials of the formed metals, however, are still limited today and controlling the detailed geometry is not an easy task. In this paper we propose a new type of extended surface based on thin metal wire, which may be considered a type of porous material. As a first step of the study we focus on one of the most basic wire structures, namely wire springs.

Use of the wire springs as extended surface has many advantages. A large surface area density can be achieved particularly when thin wires are used. Geometric parameters of wire springs such as wire diameter, cross sectional shape of wires, spring diameter, spring pitch and spring length can easily be controlled, which allows us to have many design options to achieve heat transfer requirements. There is a wide variety of material available too. If the wire diameter is small, spring fin will form a flexible structure, unlike the conventional rigid fins, which is also an advantage because such flexible structure will release the thermal stress. In addition, there is no problem for mass production and therefore it has a potential to be cost effective.

In this study, the performance of various wire springs as extended heat transfer surface is experimentally investigated at relatively low Reynolds number conditions. Fundamental data such as averaged Nusselt number and friction factor of those spring fins are accumulated and their effectiveness is discussed.

### EXPERIMENTAL SETUP

The experimental apparatus used in this study is schematically illustrated in Fig. 1. The apparatus has mainly three parts, the air duct including the test section, a heater and its controller and the measuring device to accumulate the time histories of fluid inlet and outlet temperature at the test section. Working fluid (Air) is supplied by a compressor. It flows through a flow meter, a rectifier, a heater and the test section, and then exits into the atmosphere. Air flow rate can be controlled by adjusting the regulator.

Figure 2 shows the test section part of the apparatus. It is a duct having a rectangular cross section. Its height,  $H$ , width,  $W$  and streamwise length,  $L$ , are 5.0, 100 and 50 mm respectively. Temperatures of fluid at both inlet and outlet of the test section are measured with total 30 K-type thermocouples with diameter of 0.1 mm, 15 at the inlet and the other 15 at the outlet, and their time histories are recorded at a sampling frequency of 5 Hz.

Averaged heat transfer coefficient of the spring fins is evaluated applying a transient Single-blow method, one of the unsteady measuring methods, while measuring the pressure drop at the test section under a steady state condition. Details of the transient method are introduced in the next section.

Unit spring that is applied as extended surface in this study has a shape shown in Fig.3. The spring outer diameter is the same as the duct height (5mm), which means that there is only one layer of the springs in the test section. Spring length is also fixed at 50 mm throughout this study, therefore, total 20 springs are placed inside the test section. Spring pitch,  $p$ , and the wire diameter,  $d$ , are the controlling parameters.

The geometric parameters of the spring fins examined in this study are summarized in Table 1. The symbol "03\_04" in this table, for example, stands for that the diameter of the wire is 0.3mm and its spring pitch is 0.4mm. Pitch ratio is the ratio of pitch over the wire diameter ( $p/d$ ). The wire diameter and spring pitch are varied in the ranges  $0.3 < d < 0.9$  mm and  $0.4 < p < 1.8$  mm, respectively.  $\varepsilon$  appears in the table is the porosity in the test section that is evaluated as

$$\varepsilon = 1 - \frac{V_{fin}}{WHL} \quad (1)$$

$V_{fin}$  is obtained by dividing the mass of the fins inserted in the test section with the density of the fin material (SUS304).

$A_{fin} \left( = \frac{4}{d} V_{fin} \right)$  is the surface area of the fin placed

in the test section. It is calculated assuming that a spring is a circular cylinder of diameter  $d$ . The total heat transfer area inside the test section can be expressed as

$$A_{ht} = A_{fin} + 2WL \quad (2)$$

where point contact between the spring fins and walls is assumed.

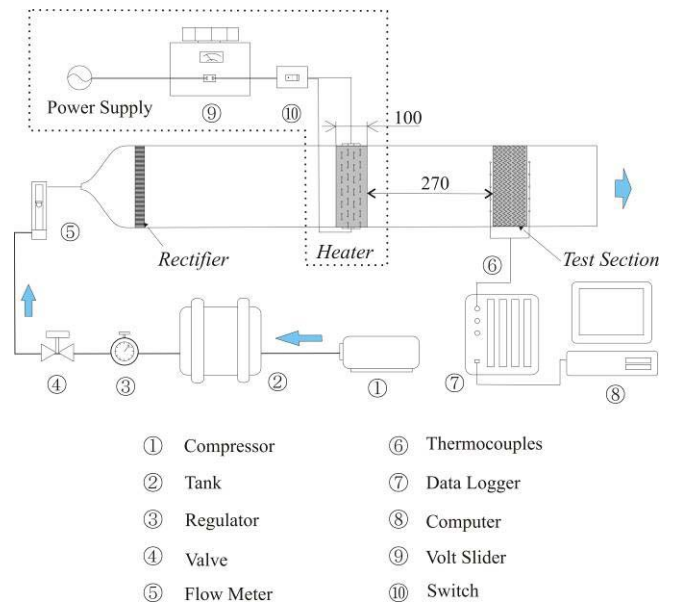


Figure 1 Experimental apparatus.

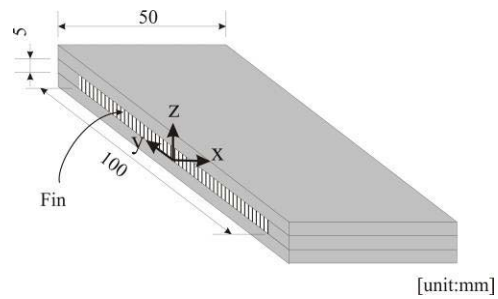


Figure 2 Test section.

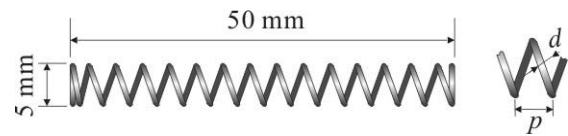


Figure 3 Spring shaped fin.

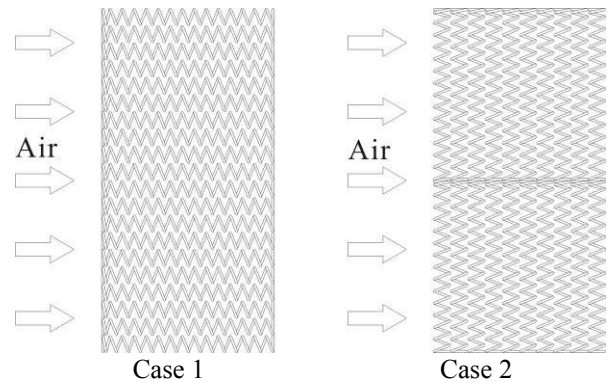


Figure 4 Spring fin arrangements in test section.

Table 1 Geometric parameters of examined spring fins.

symbol	wire diameter[mm]	pitch [mm]	pitch ratio	mass [kg]	$\epsilon$	$A_{fin}[m^2]$
03_04	0.3	0.4	1.33	0.017	0.92	0.028
03_06	0.3	0.6	2.00	0.012	0.94	0.020
03_09	0.3	0.9	3.00	0.009	0.96	0.015
03_12	0.3	1.2	4.00	0.006	0.97	0.010
03_18	0.3	1.8	6.00	0.005	0.98	0.008
05_10	0.5	1	2.00	0.018	0.91	0.018
05_12	0.5	1.2	2.40	0.015	0.92	0.016
07_12	0.7	1.2	1.71	0.031	0.84	0.023
07_14	0.7	1.4	2.00	0.029	0.86	0.021
09_12	0.9	1.2	1.33	0.045	0.78	0.025
09_18	0.9	1.8	2.00	0.033	0.83	0.018

“mass” and “ $A_{fin}$ ” are total values of 20 springs placed in test section.

Because the shape of a spring is obviously inhomogeneous, effects of spring arrangements inside the test section are expected to be large. As typical cases, two types of spring fin arrangements are employed in this study as shown in Fig.4. In Case 1, the springs are placed as the spring axis to be parallel to the main flow direction. In Case 2, on the other hand, spring axis is placed with a right angle to the main flow direction.

Characteristic length  $dh$  defined as (Manglik and Bergles, 1990)

$$dh = \frac{4\epsilon WHL}{A_{ht}} \quad (3)$$

is employed as it is often used as a characteristics length for pin fins (Brigham and VanFossen, 1984) or screen mesh (Tanaka et al. 1990). Based on this characteristic length, Reynolds number, friction factor and Nusselt number are defined as follows.

$$Re_{dh} = \frac{u dh}{\nu} \quad \text{where } u = \frac{U_0}{\epsilon} \quad (4)$$

$$f_{dh} = \frac{\Delta P}{2\rho_f u^2} \frac{dh}{L} \quad (5)$$

$$Nu_{dh} = \frac{h_{fin} dh}{\lambda_f} \quad (6)$$

## EXPERIMENTL PROCEDURE

### Single-Blow Method

Averaged heat transfer coefficient is evaluated by applying a single-blow method in this study. In this transient method, a steady flow is first established with the heater turned off and therefore all the system has a uniform temperature distribution. Then the heater is suddenly turned on so that the fluid temperature rises. From the difference between the time history of the inlet fluid temperature and that of the outlet fluid temperature, the averaged heat

transfer coefficient of the test section is figured out. The procedure is based on the following theory.

The heat input to the test section is evaluated by monitoring the fluid temperature at the inlet. The time response of the fluid temperature at the outlet depends on the heat exchange between the fluid and solid parts (fins and the wall) in the test section. Figure 5 shows typical time histories of the test section inlet and outlet temperatures measured for two different conditions. Note that the values of temperature are normalized as  $T^* = \frac{T - T_0}{T_{final} - T_0}$ , where

$T_0$  is the initial temperature and  $T_{final}$  is the inlet temperature at the end of measurement. A sharp temperature increase is observed at the inlet immediately after turning on the heater. The outlet temperatures follow it but relatively in mild ways depending on the fin performance inserted in the test section. Slower response is a sing of a larger heat exchange between the working fluid and solid parts in the test section. It shows that there is a large difference in the outlet temperature histories even the time history profiles of the inlet temperature are quite close as the cases shown in Fig.5.

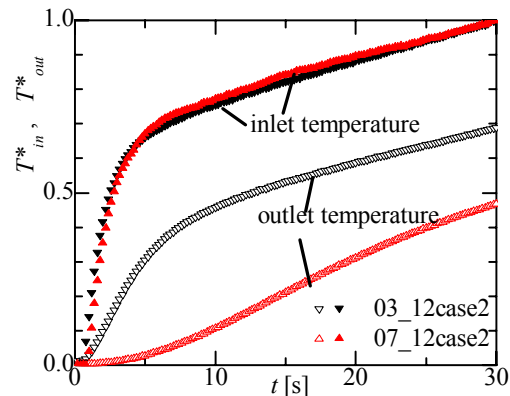


Figure 5 Typical time histories of inlet and outlet normalized temperature.

If we apply an adequate heat transfer model and provide the time history of inlet temperature as input data assuming an average heat transfer coefficient, a prediction of the time response of the fluid outlet temperature becomes possible. Consequently, by matching the predicted time response of the outlet temperature to the measured one adjusting the assumed heat transfer coefficient, we can estimate the averaged heat transfer coefficient of the test section.

### Numerical Modeling

At the early stage of the development of single-blow method, much efforts were devoted to achieve a step change of inlet fluid temperature which, however, is not an easy task because of the heat capacity of the heater itself. Lian and Yang (1975) obtained an analytical solution of the outlet temperature response when the inlet temperature change is represented by a first order time lag. Making use of this analytical solution with the aid of computers, which is known as a modified single-blow method, enabled us to avoid the difficulty to achieve a step temperature change. Reflecting the development of computer, use of single-blow based methods is recently expanding (Yagi and Mochizuki, 1990, Chang et al., 1999, Luo et al., 2001). The method applied in this study is similar to that used by Chen and Chang (1996) where the heat exchange between the fluid and the side walls are included as well as that between the fluid and the fins. The major assumptions are as follows.

1. Physical properties of the fluid and solids were constant.
2. Flow is steady.
3. Outer side of the walls is well insulated.
4. Local temperatures vary only in streamwise direction (one dimensional).
5. Heat conduction is neglected
6. There is no heat exchange between fins and walls.

The governing equations are one dimensional unsteady energy equations for working fluid, fin and walls that can be expressed in non-dimensional forms as follows:

<Fluid>

$$\frac{\partial T_f^*}{\partial t^*} + \frac{\partial T_f^*}{\partial x^*} = NTU_{fin}(T_{fin}^* - T_f^*) + NTU_w(T_w^* - T_f^*) \quad (7)$$

<Fin>

$$R_{f,fin} \frac{\partial T_{fin}^*}{\partial t^*} = NTU_{fin}(T_f^* - T_{fin}^*) \quad (8)$$

<Wall>

$$R_{f,w} \frac{\partial T_w^*}{\partial t^*} = NTU_w(T_f^* - T_w^*) \quad (9)$$

where,

$$T_f^* = \frac{T_f - T_0}{T_{final} - T_0} \quad T_{fin}^* = \frac{T_{fin} - T_0}{T_{final} - T_0} \quad T_w^* = \frac{T_w - T_0}{T_{final} - T_0}$$

$$x^* = \frac{x}{L} \quad t_i = \frac{\varepsilon \rho_f A_c L c_f}{\rho_f A_c U_0 c_f} = \frac{\varepsilon L}{U_0} \quad t^* = \frac{t}{t_i}$$

$$NTU_{fin} = \frac{h_{fin} A_{fin}}{\rho_f A_c U_0 c_f} \quad NTU_w = \frac{h_w A_w}{\rho_f A_c U_0 c_f}$$

$$R_{f,fin} = \frac{m_{fin} c_{fin}}{\varepsilon \rho_f A_c L c_f} \quad R_{f,w} = \frac{m_w c_w}{\varepsilon \rho_f A_c L c_f}$$

These equations are numerically solved until a set of  $NTUs$  are obtained under the initial and boundary conditions shown below.

<Initial condition>

$$t^* = 0 \quad T_f^*(0, x^*) = T_{fin}^*(0, x^*) = T_w^*(0, x^*) = 0$$

<Boundary condition>

$$x^* = 0 \quad T_f^*(t^*, 0) = 0$$

$T_f^*$  in the boundary condition is the normalized inlet temperature obtained in the experiment. Note that it is not necessary to be expressed as a first order time lag because in this study the above equations are numerically solved for every experimental run.

An overall picture of the employed method is schematically illustrated in Fig.6. Time histories of both inlet and outlet temperature are experimentally accumulated. The eqs. (7-9) are numerically solved assuming  $NTU_{fin}$  and  $NTU_w$ . In the numerical process, the measured inlet temperature is used as the boundary condition. The numerically predicted outlet temperature is compared with the measured outlet temperature response and if they match well, the assumed  $NTUs$  are judged to be a solution. If they do not match the values of  $NTUs$  are renewed and the same procedure repeats until a converged solution is obtained.

There are several ways to evaluate if the two response curves, that are numerical one and measured one, match or not, such as maximum slope method, five point matching, initial rise method etc. These methods are rather simple and easy to be applied, but use only limited part of the obtained data. In this study a method known as a direct curve matching is employed where the entire response curve during the measuring time interval is compared with the numerical counterpart. A mean residual of the following form is introduced and  $NTUs$  are adjusted so that the mean residual is minimized.

$$e = \left( \frac{\sum (T_{f,meas.} - T_{f,th.})^2}{N} \right)^{0.5} \quad (10)$$

The value of residual is affected by the measuring time interval. Too short or too long measuring time interval tends to increase the residual. After a series of test experiments, the time interval was fixed at 30 seconds throughout this study. Under this measuring interval, mean residual

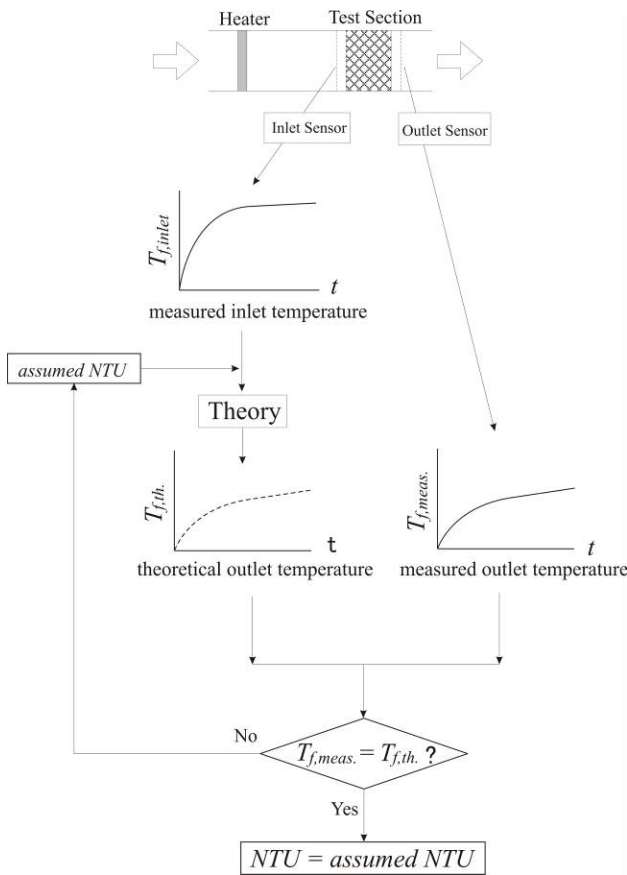


Figure 6 Flowchart of Single Blow Method.

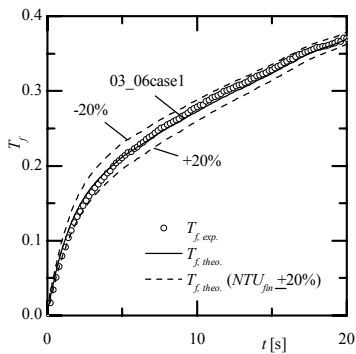


Figure 7 Comparison of predicted outlet temperature with experimentally obtained data.

typically takes a value around 0.1 degree, and the increase of the inlet temperature is typically 10 degrees depending on the flow rate. In addition to the evaluation by the residual, there is one more limiter employed in this study that is the normalized outlet temperature at the end of measuring time interval. If it is less than 0.3, the experimental data was not considered valid. This is to avoid the inclusion of less reliable data to discussion, because the too small temperature increase at the outlet should be suffering the problem of temperature measurement accuracy. The outlet temperature prediction also becomes less sensitive to the

change of  $NTUs$ , in the cases where the actual  $NTUs$  take large values.

Figure 7 is an example comparing the numerically predicted outlet temperature profile to that is obtained in experiment. Solid line shows the converged prediction and  $NTUs$  used in this calculation were employed as the final results. Two broken lines in the figure show numerical results obtained by setting the  $NTU_{fin}$  to be 20 percent larger or smaller than the solid line case. Their deviation from the experimental data can clearly be confirmed. Larger  $NTU$  leads a slower time response of the outlet temperature.

## RESULTS AND DISCUSSIONS

To assess the experimental procedure, an offset fin, commercially available, is inserted in the test section and both heat transfer and pressure drop measurements were conducted. The obtained results were compared with the empirical formula proposed by Manglik and Bergles (1990). Figure 8 shows  $j$  factor and friction factor for the offset fin. In the figure, it seems the agreement of the present  $j$  factor with the empirical formula is good enough to discuss the heat transfer performance. The friction factor obtained shows an even better agreement with that of the empirical formula as shown in the figure. These comparisons validate a discussion based on the experimental data obtained in this study. The obtained data of offset fin is used as a reference in the latter figures to evaluate the performance of spring fins.

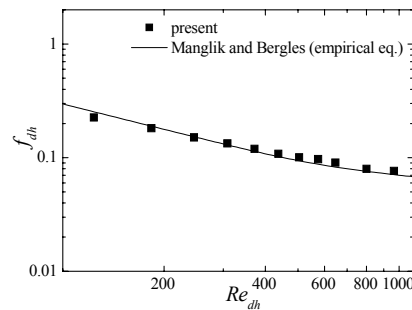
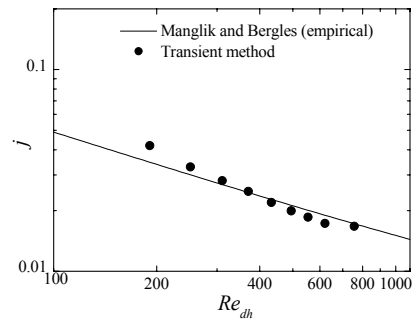


Figure 8  $j$ -factor and friction factor of offset fin experimentally obtained.

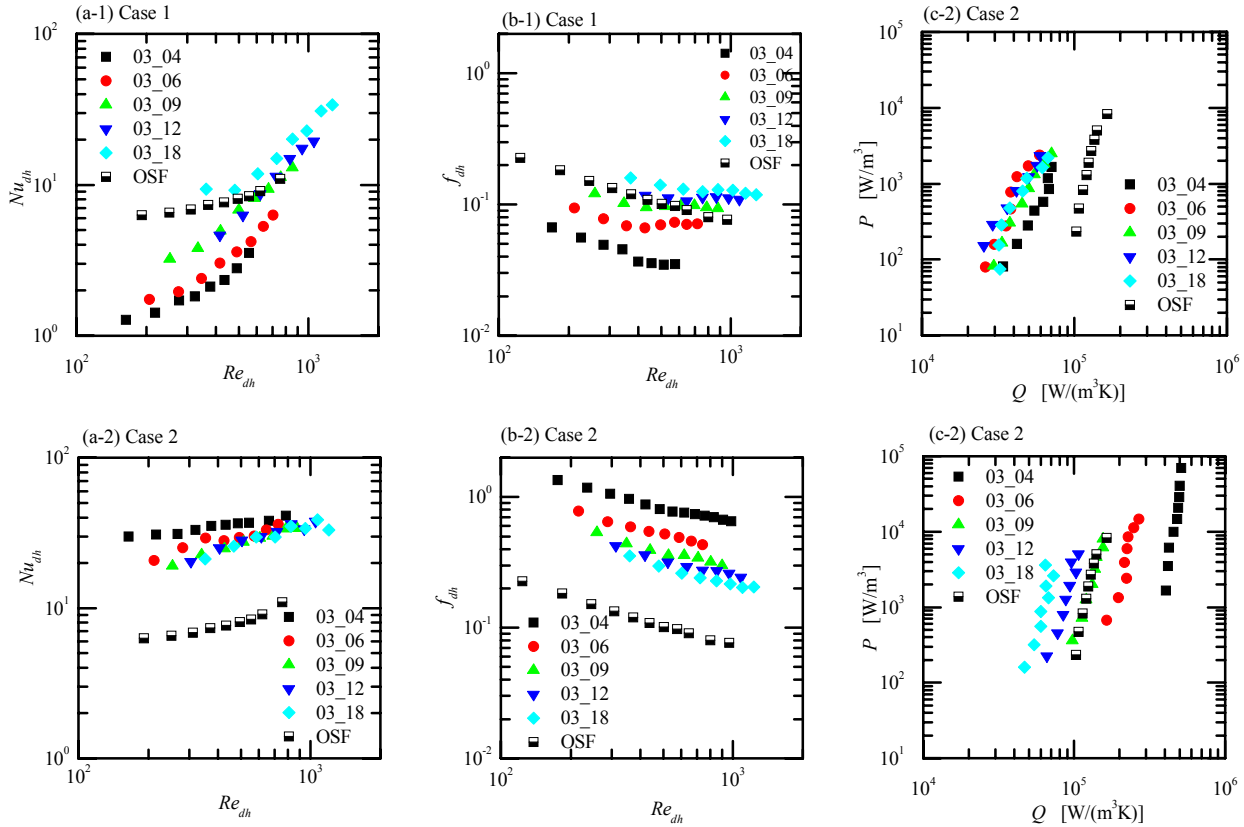


Figure 9 Spring fin performance evaluation (Constant wire diameter,  $d=0.3$  mm).

Figure 9 compares (a) Nusselt number, (b) friction factor and (c) heat transfer rate per unit volume,  $Q$ , in terms of the pumping power,  $P$ , for spring fins having wire diameter of 0.3 mm. (a-1) to (c-1) are for Case 1 arrangement while (a-2) to (c-2) for Case 2.  $P$  and  $Q$  in figure (c) are defined as follows.

$$P = \Delta P \frac{U_0 A_c}{V} = \frac{\mu^3}{2\rho_f^2} \frac{f_{dh} Re_{dh}^3}{d_h^3} \frac{A_{ht}}{V} \quad (11)$$

$$Q = \frac{h A_{ht}}{V} = \frac{h_{fin} A_{fin} + h_w A_w}{V} \quad (12)$$

In each figure, results of offset fin (OSF) are included as a reference. As the wire diameter is constant, larger spring pitch corresponds to a larger porosity and less fin surface area.

It is shown that the spring arrangement strongly affects the performance of spring fins. In Case 1, larger spring pitch results in larger  $Nu_{dh}$  and  $f_{dh}$ , that is completely opposite in Case 2.  $Nu_{dh}$  in Case 1 shows clear dependency on  $Re_{dh}$  but it is not significant in Case 2 taking almost constant values. The values of  $Nu_{dh}$  and  $f_{dh}$  in Case 1 are generally comparable or less than OSF while they take much higher values in Case 2 at any studied  $Re_{dh}$ . Fig.9(c-1) and (c-2) show that heat transfer performance OSF is always better than that obtained with Case 1 arrangement, when it is evaluated in terms of pumping power. In Case 2 arrangement, on the other hand, there are cases which achieve larger heat transfer rate than OSF at a constant pumping power. In Fig.9 (a-2)  $Nu_{dh}$  shows small

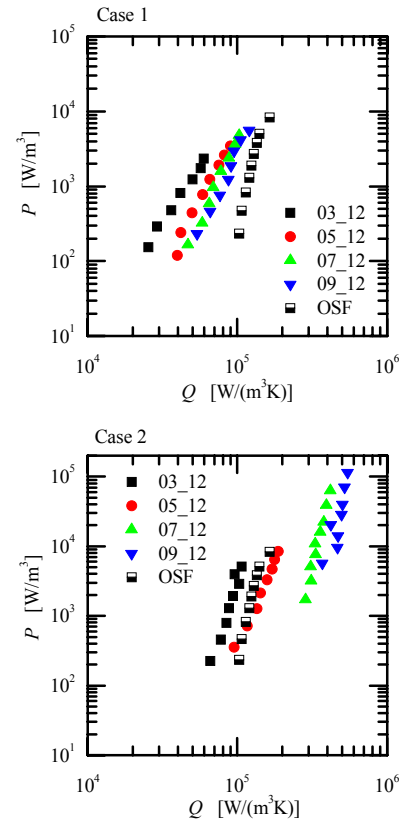


Figure 10 Spring fin performance evaluation (Constant pitch,  $p=1.2$  mm)

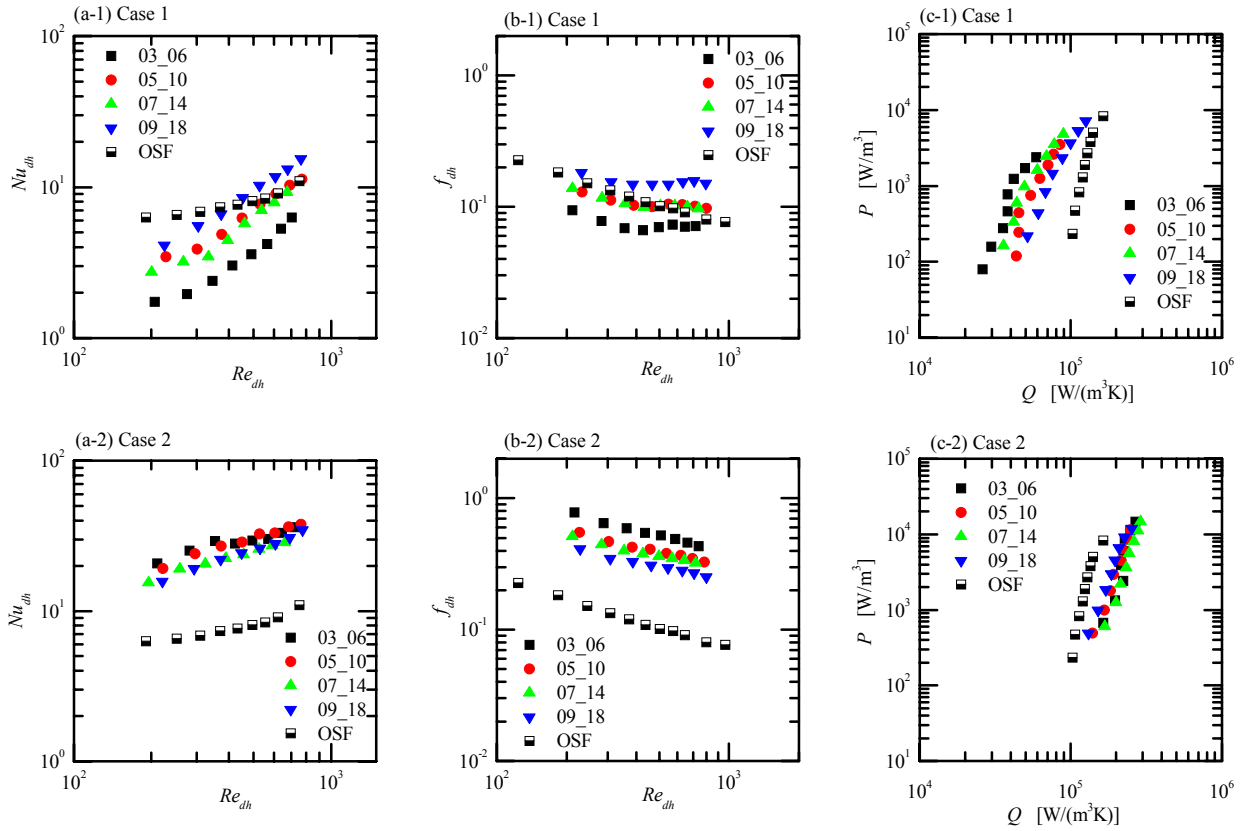


Figure 11 Spring fin performance evaluation (Constant pitch ratio,  $p/d = 2.0$ ).

dependency on the spring pitch.  $Q$  dependency on spring pitch in Fig.9(c-2) is mainly due to the difference in fin surface area.

Similar performance evaluations are shown in Figs.10 and 11. Figure 10 compares spring fins having same spring pitch,  $p=1.2$  mm. In this case pitch ratio and porosity become smaller as the wire diameter increases. Figure 11 compares spring fins having same spring pitch ratio,  $p/d=2.0$ . Porosity takes smaller value for springs with larger wire diameter.  $Nu_{dh}$  and  $f_{dh}$  for constant pitch cases are omitted for space limitation. Above discussion for Fig.9 is generally valid for these figures. None of the spring fin having Case 1 arrangement reaches to the OSF performance. Though the pressure loss penalty is relatively mild in Case 1 arrangement, heat transfer coefficient is also low and therefore fin surface area is not effectively used. A further investigation for details of flow and thermal fields is needed to discuss the reason for these features of spring fins, but one possibility is that the spring wire is covered by the thermal boundary developed upstream part of the spring itself in Case 1 arrangement.

It seems that the pitch ratio is an important parameter in Case 2. In Fig.11(c-2), all data points closely fall in one line. Furthermore, the spring fins which show better performance than OSF in Fig.9(c-2), Fig.10 Case 2 and Fig.11(c-2), have pitch ratio less than 2. Spring fins having smaller pitch ratio tend to show preferable performance.

## CONCLUSIONS

Use of thin metal wire structures as of extended heat transfer surface is proposed. The performance of various wire springs is experimentally investigated at relatively low Reynolds number conditions. Averaged heat transfer coefficient is evaluated by Modified-Single Blow method while the pressure drop is measured at a steady state. The major conclusions are as follows.

1. The arrangement of spring fins in the test section has a large impact on their performance and can totally change its heat transfer characteristics even the same springs are used. Case 2 arrangement generally showed preferable performance compared with Case 1.
2. The geometric parameters of the spring fins such as wire diameter, spring pitch, spring pitch ratio affect its performance as extended surface. In Case 2 arrangement, pitch ratio seems to be an important parameter governing its performance.
3. There are some spring fins which show better heat transfer performance than a conventional offset fin when they are evaluated in terms of the total heat transfer at a constant pumping power.

## NOMENCLATURE

$A_{fin}$  : Fin surface area [m<sup>2</sup>]  
 $A_w$  : Wall surface area [m<sup>2</sup>]  
 $A_c$  : Cross sectional area of test section [m<sup>2</sup>]  
 $A_{ht}$  : Total surface area [m<sup>2</sup>]  
 $c$  : Heat capacity [J/(kg K)]  
 $dh$  : Hydraulic diameter [m]  
 $d$  : Wire diameter [m]  
 $f_{dh}$  : Friction factor  
 $H$  : Channel height of test section [m]  
 $h$  : Mean heat transfer coefficient [W/(m<sup>2</sup> K)]  
 $j$  :  $j$  factor =  $Nu/(RePr^{1/3})$   
 $L$  : Streamwise length of test section [m]  
 $m_f$  : Mass flow rate [kg/s]  
 $m_{fin}$  : Mass of fin [kg]  
 $m_w$  : Mass of wall [kg]  
 $NTU$  : Number of transfer unit of fin  
 $Nu_{dh}$  : Averaged Nusselt number  
 $\Delta P$  : Pressure drop [Pa]  
 $P$  : Pumping power per volume [W/m<sup>3</sup>]  
 $Pr$  : Prandtl number  
 $p$  : Spring pitch [m]  
 $Re_{dh}$  : Reynolds number based on  $dh$ , =  $u dh/\nu$   
 $T_0$  : Initial fluid temperature [K]  
 $T_{final}$  : Fluid inlet temperature at the end of measurement [K]  
 $T$  : Temperature [K]  
 $T_{in}$  : Fluid temperature at test section inlet [K]  
 $T_{out}$  : Fluid temperature at test section outlet [K]  
 $t$  : Time [s]  
 $u$  : Fluid mean velocity in test section =  $U_0/\varepsilon$   
 $U_0$  : Fluid mean velocity at test section inlet [m/s]  
 $V$  : Volume of test section =  $WHL$   
 $W$  : Width of test section [m]  
 $\varepsilon$  : Porosity in test section  
 $\lambda$  : Thermal conductivity of fluid [W/(m K)]  
 $\mu$  : Viscosity of fluid [Pa s]  
 $\nu$  : Kinetic viscosity of fluid [m<sup>2</sup>/s]  
 $\rho$  : Density [kg/ m<sup>3</sup>]

subscript

$f$  : Fluid  
 $fin$  : Fin  
 $w$  : Wall

superscript

\* : Non dimensional value

## Acknowledgement

This study is partially supported by Japan Science and Technology Agency (JST) as a research in CREST project “Micro Gas Turbine and Solid Oxide Fuel Cell Hybrid Cycle for Distributed Energy System”, and by the Ministry of Education, Science, Sports and Culture, Grant-in-Aid No.16760154.

## REFERENCES

Brigham, B.A., and VanFossen, G.J., 1984, Length to Diameter Ratio and Row Number Effects in Short Pin Fin Heat Transfer, *J. Engineering for Gas Turbines and Power*, Vol. 106, pp. 241-245.

Chang, Z.C., Hung, M.S., Ding, P.P., and Chen, P.H., 1999, Experimental evaluation of thermal performance of Gifford-McMahon regenerator using an improved single-blow model with radial conduction, *Int. J. Heat Mass Transfer*, Vol.42, pp. 405-413.

Chen, P.H., and Chang, Z.C., 1996, An improved model for the single-blow measurement including the non-adiabatic side wall effect, *Int. Comm. Heat Mass Transfer*, Vol. 23, No. 1, pp. 55-68.

Chen, P.H., Chang, Z.C., and Huang, B.J., 1996, Effect of oversize in wire-screen matrix to the matrix-holding tube on regenerator thermal performance, *J. Cryogenics*, Vol. 36, pp. 365-372.

Iwai, H., Watanabe, H., Tatsumi, K., and Suzuki, K., 2003, Conjugate heat transfer for a minimal unit model of counter flow type corrugated primary surface heat exchangers, *International Journal of Heat Exchangers*, Vol.4 No.1, pp. 1-26.

Kim, S.Y., Paek, J.W., and Kang, B.H., 2000, Flow and Heat transfer correlations for porous fin in a plate-fin heat exchanger, *ASME J. Heat Transfer*, Vol. 122, pp. 572-578.

Lian, C.Y., and Yang, W.J., 1975, Modified Single-Blow Technique for Performance Evaluation on Heat Transfer Surfaces, *J. Heat Transfer*. Ser.C,97, pp. 16-21.

Luo, X., Roetzel, W., and Ludersen, U., 2001, The single-blow transient testing technique considering longitudinal core conduction and fluid dispersion, *Int. J. Heat Mass Transfer*, Vol. 44, pp. 121-129.

Manglik, R.M., and Bergles, A.E., 1990, The thermal-hydraulic design of the rectangular offset-strip-fin compact heat exchanger. *Compact Heat Exchangers* (Edited by R.K.Shah, A.D.Kraus and D. Metzger), Hemisphere, pp. 123-149.

McDonald, C.F., 2000, Low-cost compact primary surface recuperator concept for microturbines, *Applied Thermal Engineering*, Vol. 20, pp. 471-497.

Suzuki, K., and Iwai, H., 2003, High Performance Recuperators for the Solid Oxide Fuel Cell-Micro Gas Turbine Hybrid System, *Proc. of 4th International Conference on Compact Heat Exchangers and Enhancement Technology for the Process Industries*, pp. 197-203.

Tanaka, M., Yamashita, I., and Chisaka, F., 1990, Flow and Heat Transfer Characteristics of the Stirling Regenerator in an Oscillating Flow, *JSME International Journal*, Series II, Vol. 33, pp. 283-289.

Yagi, Y., and Mochizuki, S., 1990, Development of a Modified Single-Blow Method (An Application to Parallel Plate Heat Transfer Surfaces), *JSME*, B, Vol.56, No.529, pp. 2724-2728, (in Japanese).